ICANS-XI International Collaboration on Advanced Neutron Sources
KEK, Tsukuba, October 22-26, 1990

Total performance of LAM-80ET

Kazuhiko Inoue[1], Toshiji Kanaya[2], Yoshiaki Kiyanagi[1], Susumu Ikeda[3], Kaoru Shibata[4], Hirokatsu Iwasa[1], Takashi Kamiyama[4], and Yoshinobu Izumi[o,5]

1)Department of Nuclear Engineering, Faculty of Engineering, Hokkaido University, Sapporo, Hokkaido 060, Japan
2)Institute for Chemical Research, Kyoto University, Uji, Kyoto-fu 611, Japan
3)BSF, National Laboratory for High Energy Physics, Tsukuba-shi, Ibaraki-ken 305, Japan
4)Institute for Material Research, Tohoku University, Sendai, Miyagi-ken 980, Japan
5)Macromolecular Research Laboratory, Faculty of Engineering, Yamagata University, Yonezawa, Yamagata-ken 992, Japan

Abstract

Application of mica in the crystal analyser of time-of-flight spectrometer installed in a pulsed cold neutron source is a new approach in high resolution neutron spectroscopy. We constructed a new set of mica crystal analysers for the neutron spectrometer at KENS (KEK), that gave a desirable performance of energy resolution accompanying by a surprisingly sharp rise shape of resolution function. The latter characteristic was especially indicative of the usefulness of mica crystal analyser in the quasielastic neutron scattering studies of localized random motions in condensed matters.

I. INTRODUCTION

Quasielastic neutron scattering is a very useful method to study diffusive motion or the relaxation process in molecular science and in many other fields. Measurements of quasielastic scattering often require a wide energy transfer range of several orders of magnitude in addition to a relatively wide momentum transfer range. It is easily seen that the design of a single quasielastic spectrometer which has the capacity to cover such a wide energy transfer range is beyond reach. Therefore, adopting a single design philosophy, we designed three quasielastic spectrometers which can be complementary devices, and installed them at the KENS spallation cold neutron source at the National Laboratory for High Energy Physics (KEK), Tsukuba.

During the past decade we have been engaged in developing the KENS spallation cold neutron source and a high resolution quasielastic spectrometer in addition to a conventional resolution one using the pulsed cold source. Our previous studies revealed the 20 K solid methane moderator to be the most adaptable to the modest capacity accelarator-based cold neutron source of the KENS-I size. Using the pulsed cold source, we have been accumulating basic data on the performance of the quasielastic spectrometer.

Based on our accumulated information, we then constructed a pulsed cold neutron source of the KENS-I' size. Several years of successful operation have proved that the 20 K solid methane cold source is still adaptable even for the neutron source of the KENS-I' size. Furthermore, our data has revealed that the crystal analyser type time-of-flight spectrometer, combined with the pulsed cold source, is the simplest but most suitable device for quasielastic scattering because of its flexibility of performance.

This paper describes the design and the performance of the LAM-80ET, which is an improved version of the LAM-80 having the special feature of a wide energy window. The design considerations of the instrument are discussed in section Ⅱ, and the description of spectrometer and the practical performance are given in sections Ⅲ and Ⅳ. Finally, a short remark of the method of data analysis is given in section Ⅴ.

Ⅱ. Design considerations

In order to carry out quasielastic neutron spectroscopy using the pulsed cold source, it is most desirable that the neutron pulse emitted from the cold source be utilized directly for energy analysis using the time-of-flight technique without any auxiliary device for narrowing the pulse width. As to accompanying secondary energy analysing devices, there are several options. Our early results suggested that a wide acceptance angle crystal analyzer mirror is the most suitable one. Therefore, we adopted the arrangement of devices shown in fig. 1.

In the case of time-of-flight measurements, the high resolution required is attained by selecting appropriately the length of a neutron flight path to the width of the neutron pulse, the Bragg angle and the material of the analyser mirror. An appropriate selection of these combinations enabled us to design a high resolution spectrometer with high intensity. Neutron guide tube was used for the purpose of the high intensity.

Ⅱ.1 Scattered neutron spectrum

If the design parameters of the spectrometers are appropriately selected, the time spectrum of the scattered neutrons from the sample at a scattering angle θ is simply expressed as follows.

$$\eta(t;\theta)=\text{const}\int\int\phi[E_1,t-l_2/(2E_2/m)^{1/2}]\sigma(E_1\rightarrow E_2,\theta)R(E_2)dE_1dE_2 \quad (1)$$

where $\phi(E_1,t_1)$ is the incident neutron flux at time t_1 into the sample, $\sigma(E_1\rightarrow E_2,\theta)$ is the incoherent differential scattering cross section, $R(E_2)$ is the energy resolution function of the crystal analyser mirrors, m is the neutron mass, and l_2 is the average flight path length of the scattered neutrons.

The quantities measured are the energy transfer, ε, and the scattering vector, Q, defined by

$$\varepsilon = E_1 - E_2, \quad (2) \quad \text{and} \quad Q = k_1 - k_2, \quad (3)$$

where k_1 and k_2 are the wave number vectors of the incident and the scattered neutrons, respectively, and Q^2 is given as follows,

$$Q^2=(2m/h^2)[E_1+E_2-2(E_1E_2)^{1/2}\cos\theta]. \quad (4)$$

Ⅱ.2 Time-of-flight measurement

The time and energy spectrum, $\phi(E_1,t_1)$, of the neutrons impinging on the sample depends on the neutronic performance of the pulsed cold source. Since we needed precise information about the time structure of the neutron pulse emitted from the cold moderator, we measured the time structure by a thermica monochromator for the 20 K methane cold moderator and the pulse data were corrected for the monochromator resolution using the QUESA-40 code. Fig. 2 shows the pulse width at half-maximum, Δt_z, as a function of neutron wavelength after the correction of the resolution. A tremendous increase of pulse width occurs in the cold neutron wavelength range.

The energy resolution, ΔE_1, in the time-of-flight experiments is given by

$$\Delta E_1=2E_1\Delta t_z/t_1. \quad (5)$$

Using the data shown in Fig. 2, we can assess ΔE_1 as a function of the flight path length, l, for 4 and 6Å wavelength neutrons as shown in Fig. 3. From the figure, the length of the neutron flight path and the desired energy resolution in the case of the 20K methane pulsed cold source can be detemined. Because of the spatial limitation in the experimental hall, the length of the flight path is fixed to about 30m, and we obtain a resolution of 10μeV. This assessment is based on the QUESA-40 code.

Ⅱ.3 Analyser mirror

To attain the desired resolution and high efficiency, it is necessary to match the energy resolution in time-of-flight measurement, ΔE_1, for the energy resolution of the analyser mirror, ΔE_2, according to eqs. 1 and 2. The design of the analyser mirror which fulfills the above requirements is as follows: a large number of small mica crystal pieces are mounted on a surface with special curvatures so that all pieces satisfy the same Bragg condition. Moreover, the flight path lengths from the sample to the counter via each crystal piece must be almost the same so as not to sacrifice the energy resolution ΔE_1 due to variance of t_2. To fulfill the latter condition, a relatively long distance from the sample to the crystal piece and from the crystal piece to the counter is needed. To decide the dimensions of the analyser mirror, many factors are involved.

The resolution function of the mirrors $R(\theta_B)$ is calculated by the following equation,

$$R(\theta_B)=\int\int\int p(r,\Sigma,S)|r-\Sigma|^{-2}|\Sigma-S|^{-2}\delta[\theta_B-\theta_B(r,\Sigma,S)]dr\,d\Sigma\,dS, \quad (6)$$

where $\theta_B(r,\Sigma,S)$ is the Bragg angle determined by the positions r, Σ and S, and $p(r,\Sigma,S)$ is a factor representing efficiency due to the projection of each plane and the mosaicness of the crystals. The

integrations are performed with respect to the volume of the sample, the surface of the mirror and the plane of the diaphragm.

Fig. 4 shows a typical calculated results of $R(\theta_B)$ by eq. 6 for the case of the average Bragg angle of 80° and a 14 mm diameter and 80 mm height cylindrical sample. The result indicated that the angular spread of the Bragg angle $\Delta\theta_B$ is about 0.36°.

The energy resolution of the analyser mirror is estimated by the following expression,

$$\Delta E_2 = 2E_2[(\cot\theta_B \Delta\theta_B)^2+(\Delta\tau/\tau)^2]^{1/2}. \quad (7)$$

Here $\Delta\tau$ is the variance of the reciprocal lattice vector, τ, due to the limitation of the number of lattice planes contributing to the reflection. In our case, the second term in the brackets in the rhs of eq. 7 may be small enough to neglect as compared with the first term.

II.4 Overall resolution

Fig. 5 shows the variance of incident and scattered neutron energies ΔE_1 and ΔE_2 as a function of the Bragg angle calculated by eqs. 5 and 7 for the case of a flight path length 30m.

The overall energy resolution of the spectrometer is assessed by

$$\Delta\varepsilon = 2E[(\Delta t_z/t_1)^2 + (\cot\theta_B \Delta\theta_B)^2 + (\Delta\tau/\tau)^2]^{1/2}. \quad (8)$$

Here $E_1=E_2=E$ for quasielastic scattering.

Fig. 6 shows overall energy resolution of the spectrometer as a function of the Bragg angle for the case of flight path length 30 m. The highest resolution is attained for the backscattering condition of the analyser mirror, as seen in fig. 6. However, in this condition, the intensity of the scattered neutrons is seriously sacrificed due to the narrow band width, ΔE_2. An optimal condition is achieved by matching ΔE_1 to ΔE_2. The optimal condition for the desired performance can be found around the point where the two curves cross, as shown in fig. 5.

III. Description of spectrometer

The LAM-80ET utilizes a LAM-type analyser mirror, of which the structural frames supporting the crystal pieces were fabricated according to the same design method described previously. The average distance from the sample to the counter diaphragm via the mirror crystal is 120 cm.

III.1 High resolution machine

Fig. 7 shows the configuration of the LAM-80ET. The spectrometer is installed at the C-2 neutron guide hole, of which the distance from the cold source is about 26 m. As seen in the figure, there are eight identical mirrors, each containing 400 mica crystal pieces of 12mmx12mmx 3mm in size. Each analyser mirror is mounted at four fixed angles: ±15°, ±51.7°, ±78° and ±118°. Thus, the scattering angle of the analysers can cover the region from 15° to 118°. The set of analyser mirrors is housed in an evacuated container surrounded by neutron shields made of borated resin and cadmium sheets. Moreover, each analyser mirror has its own inner shields, as shown in fig. 7.

Fig. 8 shows bird's-eye view of the array of analysers, which

consists of eight analysers and eight helium counters. Scattering sample is placed at the center. Shieldings and diaphragms are not drawn.

Ⅲ.2 Sample container

A cylindrical shape was adopted for the scattering sample, to assure identical geometrical conditions for every analyser mirrors. The typical dimensions of the sample are 14 mm diameter and 80 mm height. These dimensions were determined by the optimization condition calculated between the energy resolution and the counting efficiency. This type of sample container proved to be very useful for liquid samples, and it could be utilized for the spectrometer at a wide temperature range of from 20 K to ambient temperature. However, a plate shape was adopted for the scattering sample in a tunneling experiment, as shown in Fig. 9, and it was utilized for the spectrometer at a wide temperature range of from 5 K to ambient temperature, in which a Heritoran was used as the cryostat.

Ⅲ.3 Data acquisition system

The system consits of three parts, that is, microcomputer, time analyser, and read/write as in the LAM-40 spectrometer. Fig. 10 shows the flow chart of the data acquisition system of the LAM-80ET.

Ⅳ. Performance

Ⅳ.1 Resolution

Fig. 11 shows diffraction peaks of mica and related crystals measured at the Bragg angle of 87° at the outlet of 31 m cold neutron guide in KENS. The peak shapes of mica are excellent for the higher order reflections from second to fifth but those of pyrolytic graphite are not as good as mica crystals for three values of mosaic spread.

Moreover, as can be seen from fig. 11, the background signal by stray neutrons scattered from the crystal is very faint in the case of mica. The reflections of mica from second to fifth are available for analysing the energy of scattered neutrons. Table 1 compiles the resolution (FWHM) of the spectrometer for each analysing energy. Here I_K is the relative intensity of the elastic peaks for each analysing energy for KENS condition.

Fig. 12 shows the measured spectra from vanadium using mica analyser of LAM-80 for E_3 and E_5 analysing energies. The shapes of the spectra indicates the usefulness of mica crystal analyser in the measurements of faint quasielastic spectrum accompanying with a strong elastic peak.

The LAM-80ET adopts the mirror of four times large size compared with that of the LAM-80. This means that the intensity gain is four times and generally the resolution is much worse. However, there is a solution, in which the intensity gain is four times compared with that of the LAM-80 but the resolution of the LAM-80 is conserved. Fig. 13 shows the typical results of the resolution function for each reflection from mica. The solid lines are the vanadium runs by the LAM-80 and the points are those obtained by the LAM-80ET. From this figure, we can see that the resolution for the LAM-80ET is almost the

same as that for the LAM-80.

IV.2 Intensity

Fig. 14 shows a comparison between the intensities obtained by using the LAM-80 and the LAM-80ET. The scattering sample was vanadium at ambient temperature. The intensity was normalized by monitor counts. We can see that the total intensity for the LAM-80ET is now eight times compared with the LAM-80 for each reflection from mica.

IV.3 Application

The LAM-80ET has been applied to study a tunnelling phenomenon, a sol-gel transition, a low energy excitation in amorphous polymers, and others. As a typical example, fig. 15 shows the tunnelling spectrum of N-oxy γ picoline measured by the LAM-80ET at 5K. The energy resolutions for these experiments are about 5 (down) and 16 μeV (up), respectively. Fig. 16 shows the temperature dependence of the tunnelling spectra of the same sample. We can easily seen that the tunnelling phenomena is observed the temperature goes down. Furthermore, a preliminary experimemnt for the energy resolution of 1 μeV has been tryed. Fig. 17 shows a typical result for N-oxy γ picoline using the (002) reflection. The measuring time was about 17 hours. Moreover, the counting rate and the resolution of the LAM-80ET have been confirmed to be comparable to those of IRIS at RAL (see Table 2).

V. Data analysis

As seen from eq.1, the measured neutron spectra are not simply related to the cross section of the sample as in the case of direct geometry facilities. Instead, they are expressed as the results of complex double convolution integrals related to the scattering function, the time structure of incident neutron pulse and the resolution of the analyser mirror. We are developing a data reduction program (QUESA-80ET code) for the determination of the scattering functions from measured spectra which consists of procedures for curve fitting of the spectra and hypothesis testing of the assumed scattering functions.

The measured spectrum is compared with calculated one in the data analysis by using QUESA-80ET code. The time-of-flight spectrum of scattered neutrons is actually expressed as a form of double integrals with respect to E_1 and E_2. In QUESA-80ET code, however, integration for the time-of-flight spectrum $\eta(t,\theta)$ is simply performed as follows

$$\eta(t,\theta) = \text{const} \int Y(t,\varepsilon)\, S(Q,\varepsilon)\, d\varepsilon, \qquad (9)$$

where $S(Q,\varepsilon)$ is the scattering function, Q is the average scattering vector and $Y(t,\varepsilon)$ is the effective resolution function given by

$$Y(t,\varepsilon) = \int \phi(E_2+\varepsilon, t - l_2/(2E_2/m)^{1/2})\{E_2/(E_2+\varepsilon)\}^{1/2} R(E_2)\, dE_2. \qquad (10)$$

For data analysis of quasielastic scattering, it is essential that multiple scattering corrections be assessed as accurately as possible by considering energy transfer and angular dependency. Some computer codes have been written for the multiple scattering calculations.

Information about neutron pulse structure is necessary to calculate the effective resolution function $Y(t,\varepsilon)$. Fig. 18 shows a

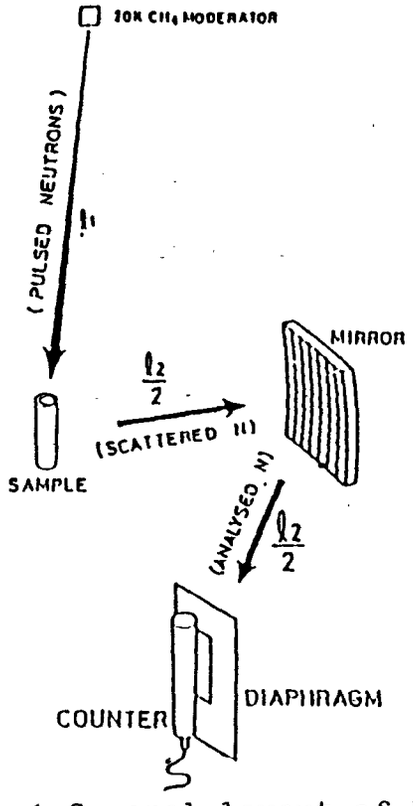

Fig.1 General layout of LAM

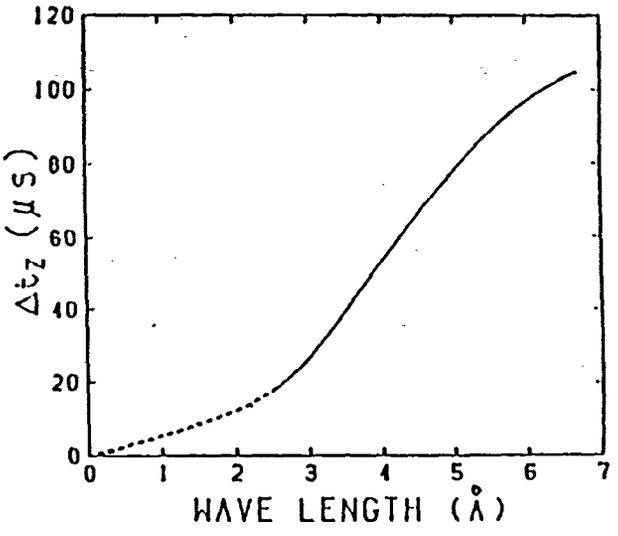

Fig.2 Measured pulse width as a function of wavelength

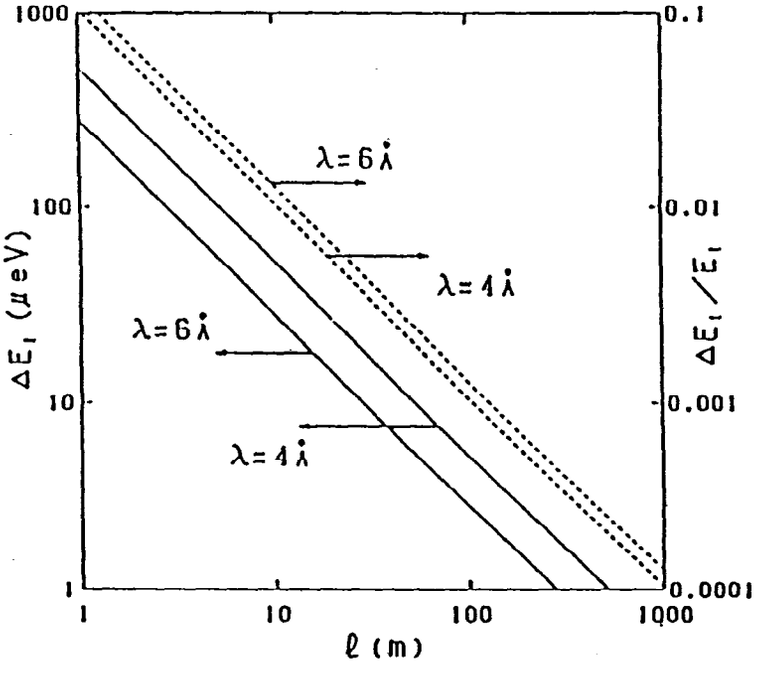

Fig.3 Total flight path length required for specified energy resolution.

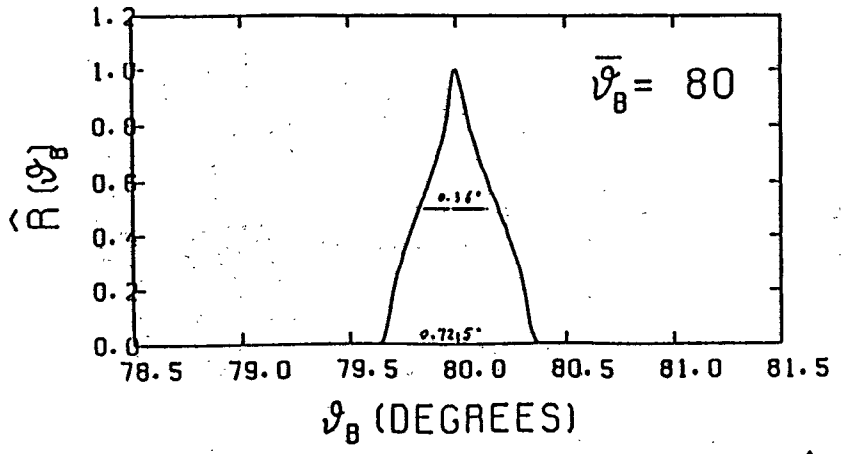

Fig. 4 A typical calculated result of $\hat{R}(\theta_B)$.

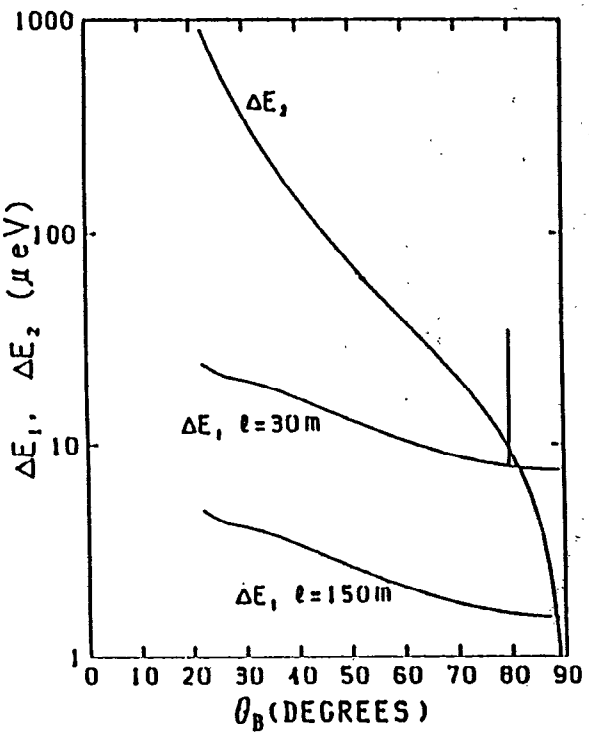

Fig.5 Partial energy resolutios as a function of the Bragg angle.

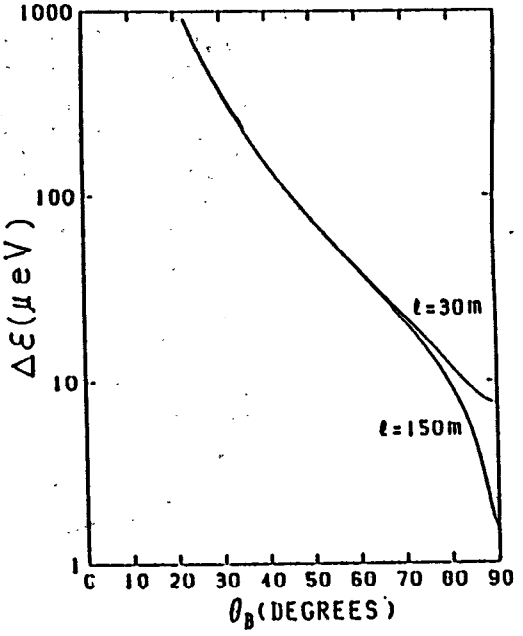

Fig.6 Overall energy resolutions

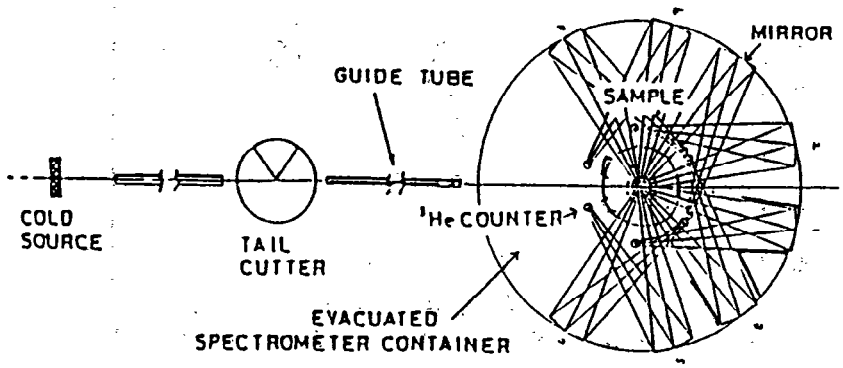

Fig. 7 The configuration of the high resolution quasielastic spectrometer (LAM-80ET)

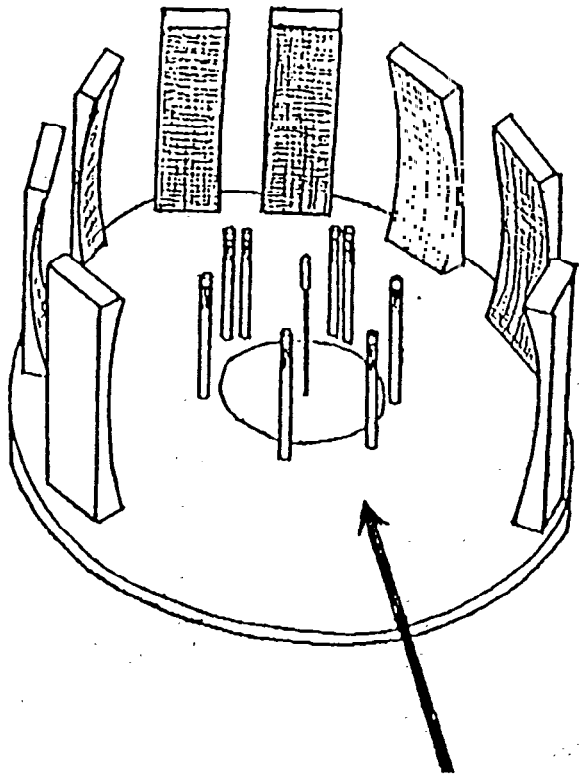

Fig. 8 Bird's-eye view of the LAM-80ET

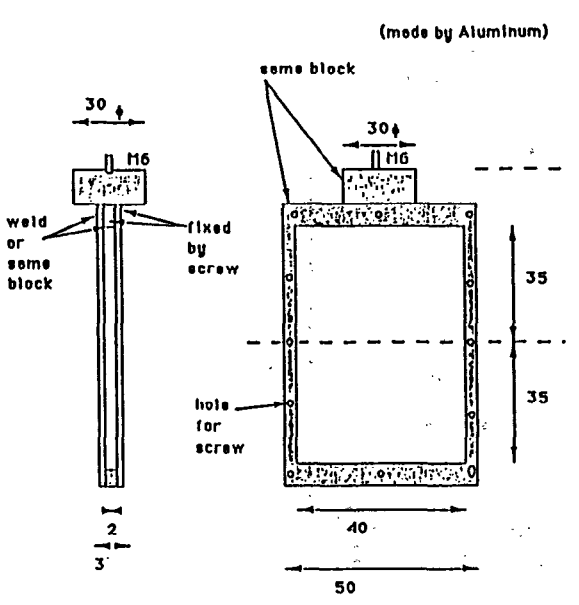

Fig. 9 Sample container for a tunneling experiment

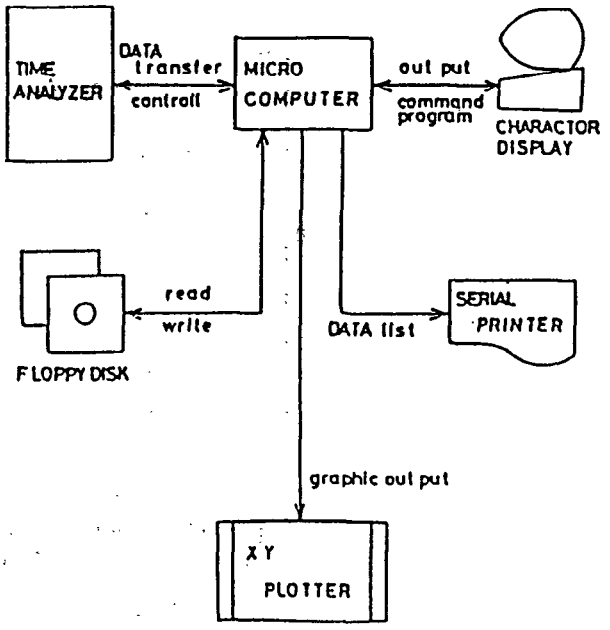

Fig. 10 Data acquisition system

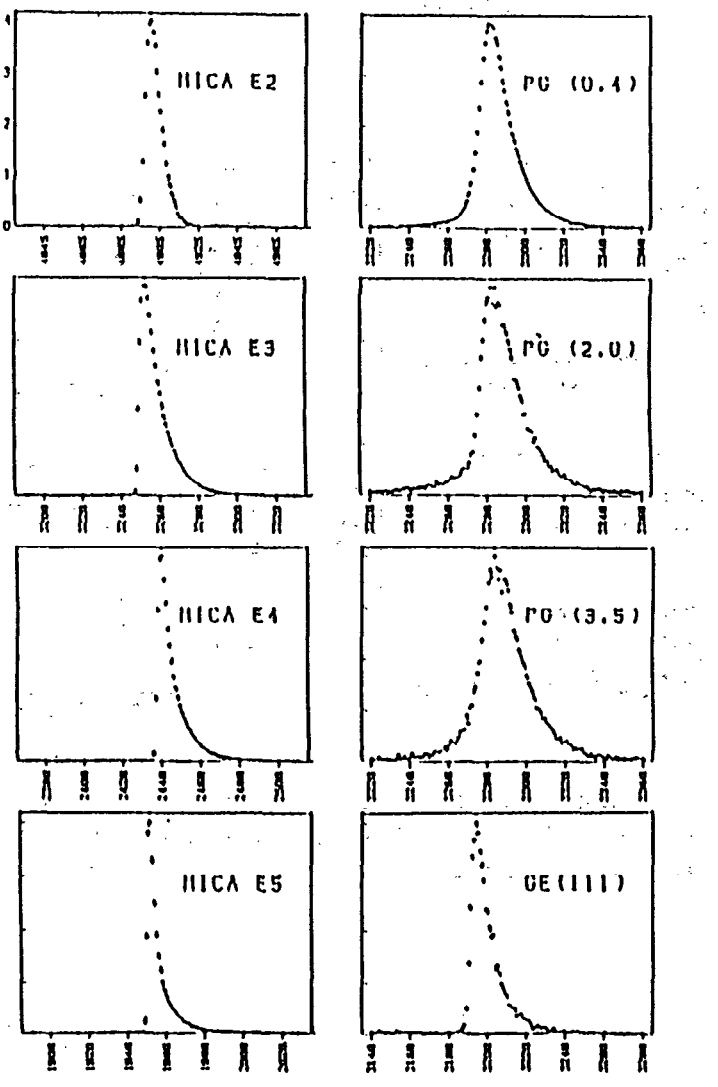

Fig. 11 Diffraction peaks of mica and related crystals

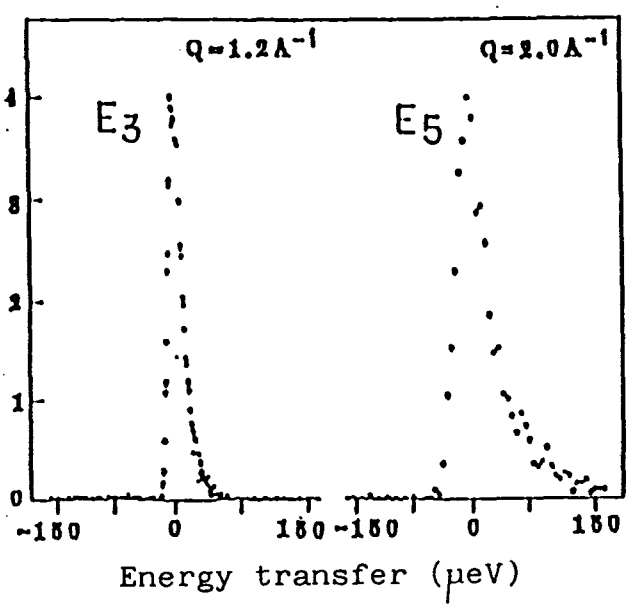

Fig. 12 Neutron scattering spectra from vanadium

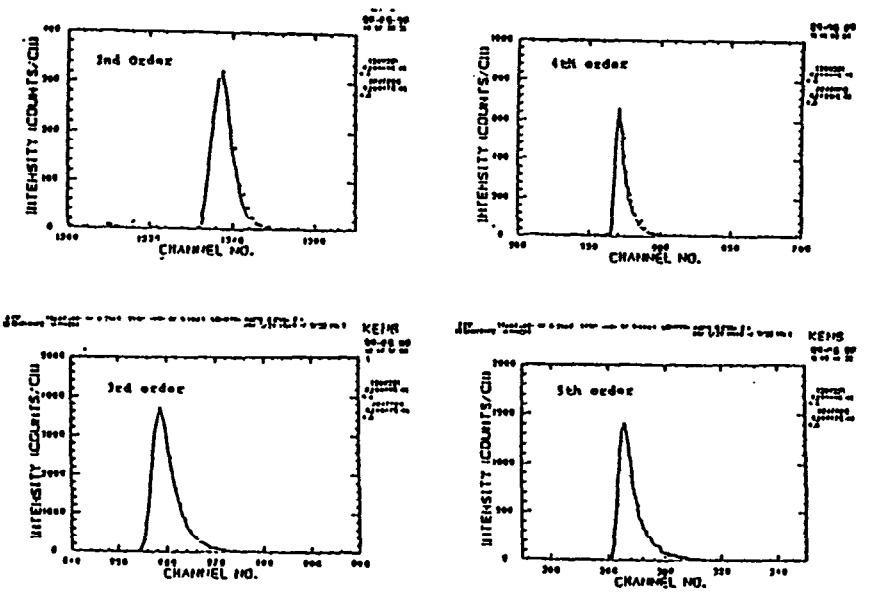

Fig. 13 A comparison between the resolution function of the LAM-80 (solid line) and the LAM-80ET (points) for each reflection.

Table 1. Parameters for each reflection

K	E_K(mev)	$\Delta \varepsilon_K$(μeV)	I_K
1(002)	0.20	1.2	
2(004)	0.83	5.5	0.08
3(006)	1.86	16	1.0
4(008)	3.31	31	0.32
5(0010)	5.18	39	0.74

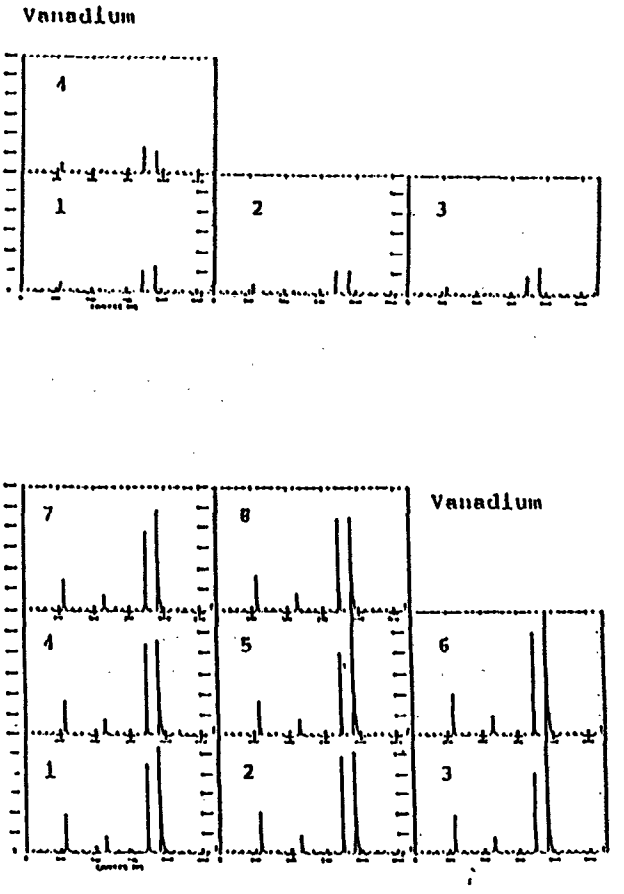

Fig. 14 A comparison between the intensities obtained by using the LAM-80(up) and LAM-80ET(down).

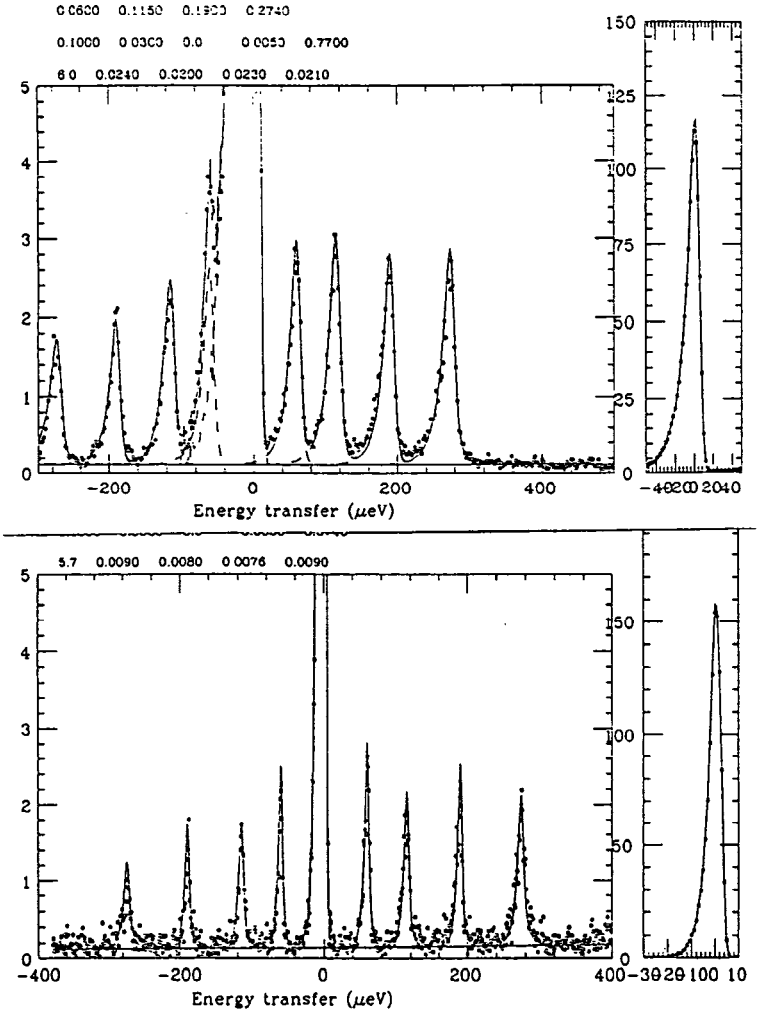

Fig. 15 Tunnel spectra of N-oxy γ picoline. The energy resolutions are 16μeV (up) and 5μeV (down), respectively.

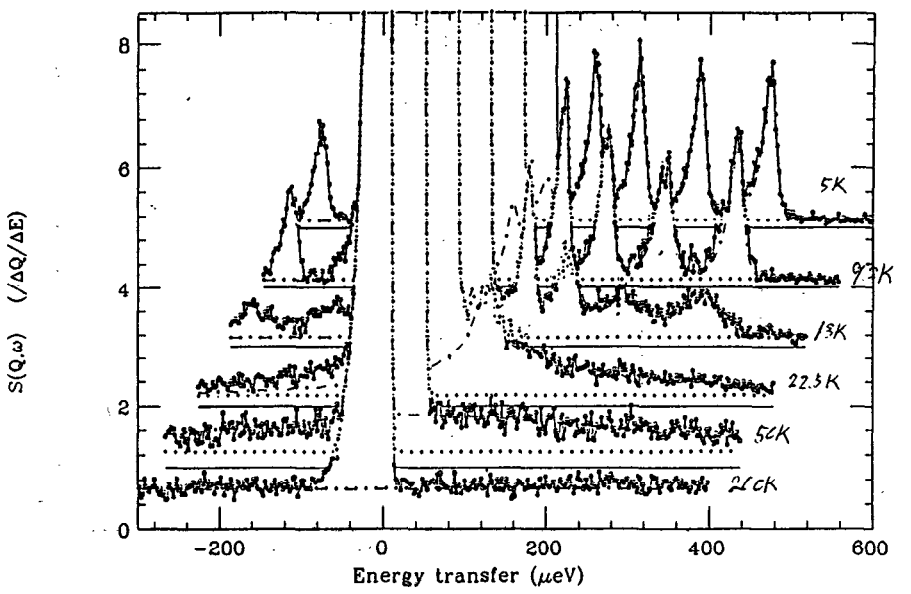

Fig. 16 Temperature dependence of the tunnel spectra of N-oxy γ picoline: the temperature cooresponds to 5, 9.2, 13, 22.5, 50 and 200K, respectively.

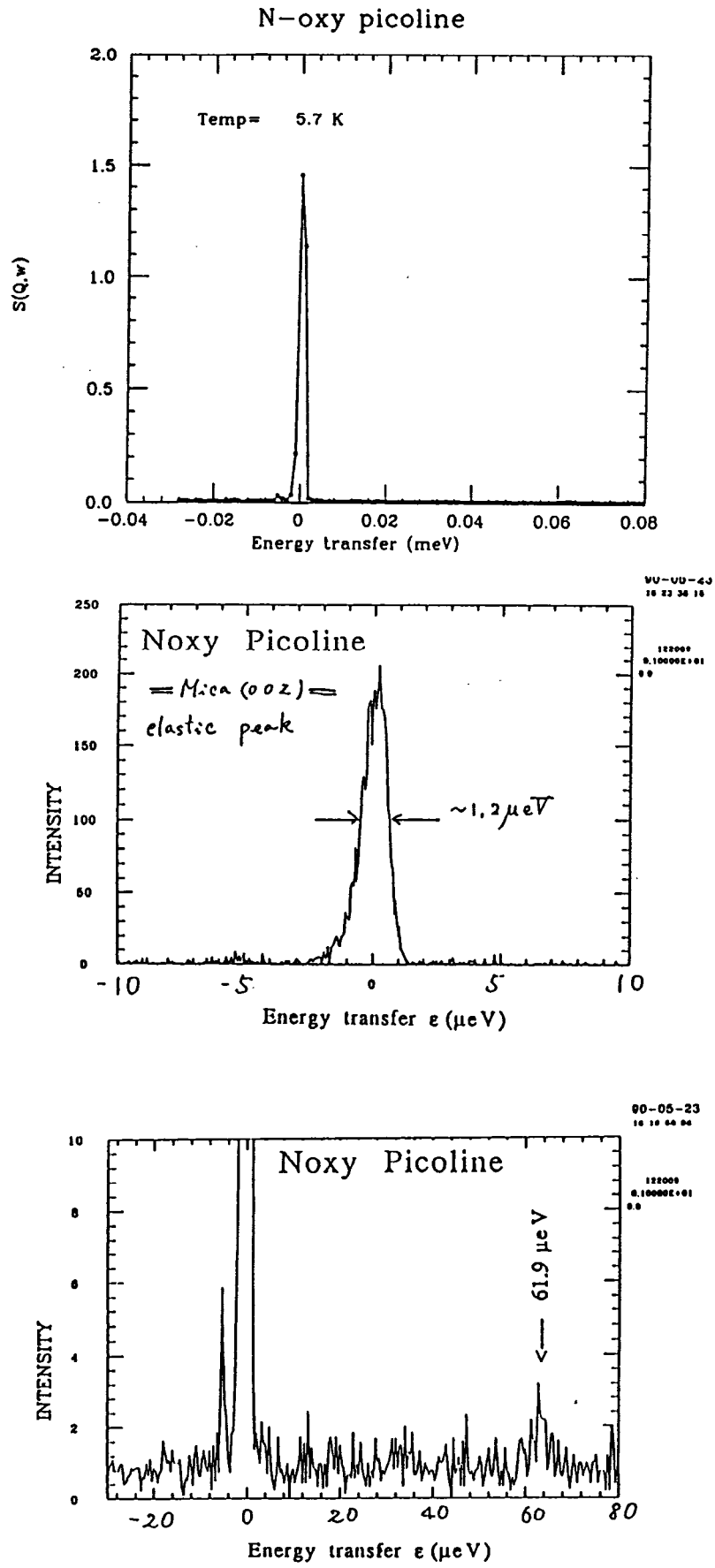

Fig. 17 Tunnel spectrum of N-oxy γ picoline. The energy resolutions is about 1μeV.

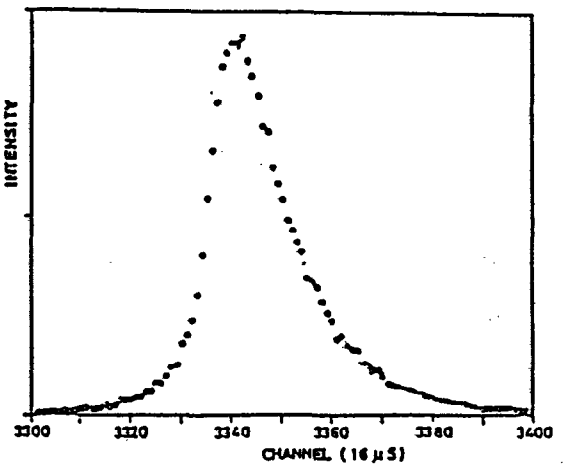

Fig. 18 Pulse structure at the place of LAM-80ET.

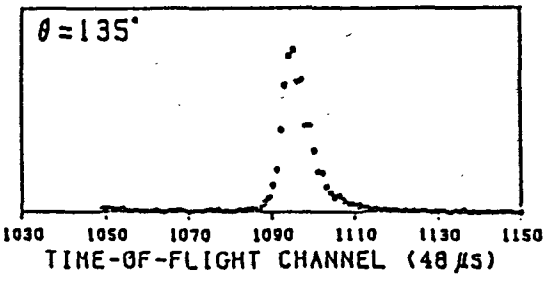

Fig. 19 Scattered spectrim from vanadium.

Table 2. A comparison of total performance between IRIS and LAM-80ET

POSITION	ITEM		IRIS	Relative Gain of IRIS against LAM-80	LAM-80ET
Source	Proton Beam	Energy (MeV)	750.	1.7	500.
		Current (μA)	100.	20.	5.
		Proton per pulse (p.p.p.)	1.3×10^{13}		1.2×10^{12}
		frequency (Hz)	50.		20.
	Moderator	Materials	Liquid H_2	1/8	Solid CH_4
		Temperature (K)	25.		20.
		Type	Cd decoupled		decoupled
		sub total		4.25	
Guide	Chopper	Window Δλ (Å)	2.		8.
		Frequency (Hz)	50.~10. (62.' disc at 6.4m)	1.	20.
	Guide Tube	Cut off (Å)	1.5		4.
		Option	Super Mirror Converging Guide	2.8	None
	Beam Size at Sample Position	(^{H} mm × ^{W}mm)	35.×25.		50.×20.
		sub total		2.8	
Spectrometer	Flight Path	L1 (m) (Source to Sample)	36.54		26.3
		L2 (m) (Sample to Counter)	1.47 (0.83+0.63)		1.2 (0.60+0.60)
	Analyzer Mirror	Area (^{H}cm × ^{W}cm)	(6.×225.)		(49.×16.8)×8
		Solid Angle (Sr)	0.196	1/9	1.83
		Crystal	P.G.	3.0	Mica
		Reflection Index	(002),(004),(006)		(002),(004),(006), (008),(0010)
		Bragg Angel (θ_B)	87.5		80.
		Type	Vertical Energy Focussing		Horizontal Energy Focussing
		sub total		1/3	
Total Gain				4.0	

preliminary data of pulse structure of cold neutrons from pulsed source at the outlet of 30 m guide tube. Fig. 18 shows the spectrum from vanadium and it is used to confirm the accuracy of the calculated effective resolution function in the case of $\varepsilon = 0$. As seen from eqs. 9 and 10, $Y(t,0)$ has a pulse shape which equals exactly to the one of elastically scattered neutrons.

VI. Conclusion

The LAM-80ET described herein has demonstrated a satisfactory performance, and it has also shown the usefulness of the 20 K methane pulsed cold source. This instrument can be used effectively to study diffusive phenomena in detail by quasielastic scattering.

We are very much indebted to the many persons who have contributed to the performance of the LAM-80ET. It is a great pleasure to thank, in particular, Prof. N.Watanabe, Dr. A.Inaba, Dr. T.Takeda, and Dr. C.J.Carlile.

References

1. T.Springer, Springer tracts in modern physics., vol. 64 (Springer, Berlin, 1972).
2. T.Springer, Topics in current physics, vol. 3 (Springer, Berlin, 1977).
3. G.E.Bacon, Neutron scattering in chemistry (Butterworths, London, 1977).
4. M.Bee, Quasielastic neutron scattering (Adam Hilger, Bristol and Philadelphia, 1988).
5. Y.Ishikawa, KENS Report-IV, National Laboratory for High Energy Physics Report, Tsukuba, Japan (1983).
6. K.Inoue, Y.Kiyanagi, H.Iwasa and Y.Sakamoto, Nucl.Instr. and Meth., 178,459(1980).
7. K.Inoue, Y.Kiyanagi and H.Iwasa, ibid., 192,129(1982).
8. K.Inoue, Y.Ishikawa, N.Watanabe, K.Kaji, Y.Kiyanagi, H.Iwasa and M.Kohgi, ibid., A238,401(1985).
9. S.Ikeda, N.Watanabe, S.Satoh, M.Furusaka and K.Inoue, KENS Report-VI,24(1985/1986).
10. K.Inoue, K.Nishida, H.Iwassa, T.Akaba and F.Hiraga, KENS Report-VI,210(1985/1986).
11. K.Inoue,S.Ikeda,Y.Kiyanagi,K.Shibata,T.Kanaya,H.Iwassa,H.Niizeki, K.Kobayashi and T.Yoshihara, KENS Report-VII,17(1987/1988).

Q(A.D.Taylor): What is the width of the INELASTIC tunneling feature in N- Oxy-γpicoline taken with 1 μeV resolution.

A(Y.Izumi): The S/N of the data in the present preliminary experiment is insufficient to estimate the width.

Q(R.Pynn): Is the secondary spectrometer evacuated?

A(Y.Izumi): Yes, it is evacuated by a rotary pump to 10^{-3} mmHg.